The Korean Journal of Rheology,
Vol. 4, No. 1, June 1992 pp.52-61

〈연구논문〉

표면성장 폴리에틸렌 섬유의 제조조건이 그 물리적 성질에 미치는 영향

노영욱 · 김상용

서울대학교 공과대학 섬유공학과

(1992년 3월 25일 접수)

Effects of the Preparing Conditions on the Physical Properties of Surface Grown UHMW PE Fibers

Young Wook Noh and Sang Yong Kim

Department of Textile Engineering, College of Engineering, Seoul National University, Seoul 151-742, Korea

(Received March 25, 1992)

요 약

초고분자량 폴리에틸렌을 파라 크실렌에 녹인 희박 용액에 전단 흐름을 가해, 섬유를 뽑아내는 방법에 대해 연구하였다. 표면성장이라 불리는 이 방법은, 용액내에서 회전하는 rotor의 표면에 흡착된 젤 층에, 결정성이 강한 씨(seed)를 접촉시킴으로써, 엉킨 분자쇄들이 전단력에 의해 신장되어 분자의 자유에너지가 증가하도록 하여 연속적으로 고강력, 고탄성률 결정을 뽑아내게 한 것이다. 이 표면성장법으로 섬유를 얻는데 있어서 결정화 온도, rotor 속도, 권취속도 및 고분자 농도와 같은 결정화 변수를 변화시키면서 섬유의 물리적 성질에 미치는 영향을 관찰하였다. 이 방법으로 섬유를 성장시키면 열역학적 평형온도(118.6℃) 이상인 120℃에서 성장시켰을 때 133 GPa의 인장 탄성계수, 3.1%의 절단신도에서 5.04 GPa의 고강력을 갖는 섬유를 얻을 수 있었다. 또한 이 방법에 있어서는 결정화 온도가 물리적 성질에 가장 큰 영향을 미치는 인자로 작용하였다. 고분자 농도의 영향은 0.7 wt.% 이상에선 물리적 성질이 더이상 개선되지 않았으며, 오히려 장력의 증가로 불안정한 성장을 보였다. 또한, 0.5 wt.% 이하에서는 젤층의 형성이 둔화됨을 볼 수 있었다. 결국 물리적 성질의 측면에서 볼 때 0.5~0.7 wt.%에서 최적 조건을 보여주었다.

Abstract—A study on the fibrous crystallization process of ultra high molecular weight polyethylene (UHMWPE) from a dilute solution subjected to a shear flow, described as "Surface Growth", has been made. The factors affecting the physical properties has been investigated by changing the crystallization variables such as crystallization temperature, rotor speed, take-up speed, and polymer concentrations. The fiber obtained by this process at a temperature above the thermodynamic equilibrium temperature (118.6℃) gave a tensile modulus of 133 GPa and a breaking stress as high as 5.04 GPa at a breaking strain of 3.1%. The crystallization temperature turned out to be the most dominant factor affecting the physical properties. The change in polymer concentrations showed no enhancement in physical properties above 0.7 wt.%, arising from the increase in tension on the fiber. Below 0.5 wt.% it is clear that there is a decrease of the gel layer formation on the rotor surface, thus giving an optimum range in view of physical properties, ranging between 0.5 wt.% & 0.7 wt.%.

Keywords: Surface growth, UHMWPE, seed crystal, thermodynamic equilibrium temperature

1. Introduction

The subject of producing polymers with ultra high modulus and strength has recently attracted great interest. New methods which can lead to enhancement in the molecular orientation and chain extension were found, thereby giving better mechanical properties. Methods like solid-state polymerization of single crystals of monomers, high pressure extrustion of solid polymers [1], solidification of polymers exhibiting liquid crystalline behaviors, prevention of chain back folding by zone drawing techniques [2-5], subsequent hot drawing of spun gels [6-8], and crystallization of polymers in elongational flow fields [9, 10] are methods to achieve high modulus and high strengtth polymers.

The approach here is to reduce the structural defects in crystalline polymers, such as chain ends, kink bands, and trapped entanglements [11], which can lower the strength and modulus of the polymer. This can be achieved by stretching very long chain molecules [12] when crystallization occurs. Basically polymer molecules crystallize when the supercooling is large, which induces lots of chain folds and chain defects, but crystallization at low supercooling can lead to more perfect structures.

The technique used in this experiment [13, 14] described as "Surface Growth Technique" allows crystallization to occur at temperatures close and even above [15] the thermodynamic equilibrium temperature (118.6℃) [16]. This method consists of sliding a seed crystal through a supercooled entanglement network that is adsorbed on the surface of a rotating rotor [17]. The gel layer of entangled chain molecules is formed by the shear flow of a dilute solution [18]. When the seed crystal comes into contact with this gel layer, longitudinal crystal growth [19] can be initiated by stretching the network in the flow field, thus producting high strength and high modulus fibers.

The purpose of this study is to investigate and explore factors which affect the physical properties, by varying the crystallization variables such as crystallization temperature, rotor speed, take-up speed, and polymer concentration, thus showing an optimum condition if any. Moreover, such a study may also add to the understanding of other routes leading to the production of ultra-high modulus polymers and to the understanding of comparable processes, like subsequent hot drawing of spun gels [6-8].

2. Experimental

2.1. Preparation of UHMW PE gel solution

All fibrillar crystals dealt with in this study were grown from a high molecular weight linear polyethylene Hostlen GUR 415. Its viscosity average molecular weight (Mv) was 7.3×10^6 and its density was 0.935 g/cm^3, supplied by Hoechst Chemicals Ltd.

For the preparation of the solution, solvent p-Xylene (b.p. 138℃) and UHMW PE was used to make concentrations of 0.4, 0.5, 0.6, 0.7, 1.0 wt.%. All solutions were stabilized by 0.5 wt.% of the antioxidant DBPC (Di-tertiary butyl para-cresol) and all experiments were carried out under purified nitrogen to prevent oxidative degradation. To achieve exact temperature measurements, an additional agitator was used for the oil bath giving temperature measurements, an additional agitator was used for the oil bath giving temperature control to better than 1℃ of the preset temperature.

2.2. Apparatus

The apparatus used throughout this experiment comprised of a teflon (PTFE) rotor placed with its axis horizontally in a cylindrical glass vessel, containing the supercooled polymer solution [20] (Fig. 1). The top was firmly sealed and was kept under purified nitrogen in order to prevent oxidative degradation. The teflon rotor had a diameter of 80 mm and its surface was slightly sand blasted for the close adhering of the gel layer. The rotor was also slightly tapered preventing overgrowth of the fibers which will result to fracture. A tensometer was attached right below the take-up device in order to measure the tension of the fiber at growth.

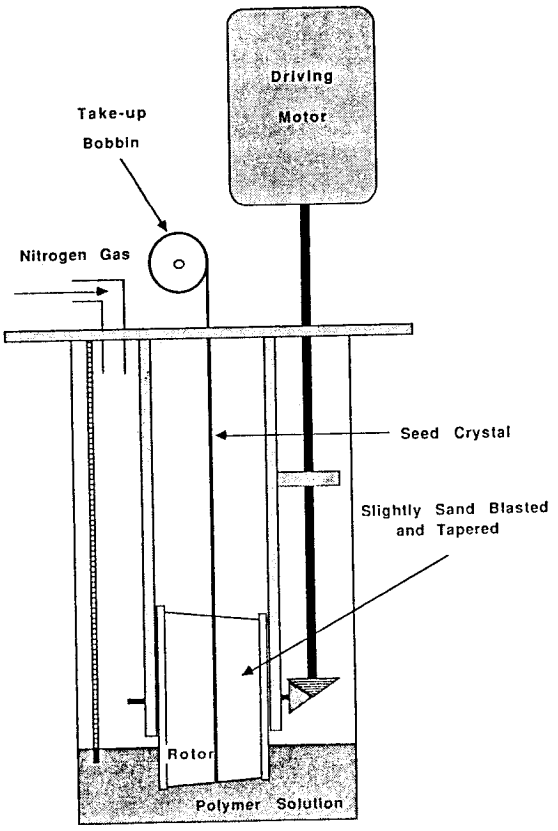

Fig. 1. Schematic diagram of surface growth apparatus.

2.3. Formation of surface grown fiber

Upon the completion of the solution, it is transfered to the apparatus. The solution must be continuosly agitated or it will lose the ability to form a coherent gel [18]. The seed crystal was prepared using a PET fiber soaked in the same solution which was then dried to form elementary crystals on the surface of the seed. The seed is then suspended in the apparatus and soon after the seed became taut at the rotor surface, the take-up device was activated to prevent overgrowth of the fiber. One remark here is that surface growth is initiated only when the seed crystal makes extremely close contact with the rotor surface, thus the seed length must be at least half the distance of the rotor circumference. Once the growth is initiated the fiber can be grown for quite a while, since the fiber has a somewhat self regulating mechanism.

2.4. Characterization

The tensile properties was measured using an Autograph IS-500 tensile tester. The sample length was 20 mm and the tensile modulus was calculated at 1.6% elongation. Birefringence was calculated by measuring the retardation of the optical path of the samples using a Nikon Optiphot-Pol polarizing microscope. The heat of fusion was determined by using a DuPont 1090DSC at a heating rate of 20℃/min.

The surface structures of the fibers were observed by using a JEOL JSM-35 scanning electron microscope. In order to calculate the orientation factor by Stein's equation [21], a Denki DMAX III-A X-ray was used performing an equatorial scanning, then an additional azimuthal scanning at a 2θ angle of 21.4°.

3. Mechanism & Macroscopic Structure

The mechanism underlying the formation of the ultra high strength and modulus of UHMW PE by means of the surface growth technique is as follows.

As the seed crystal makes contact with the gel layer on the rotor surface, the adsorbed polymer molecules make loops extending into the solution and other moleucles become entangled with those loops and with each other. Thus a network with physical crosslinks adheres to the rotor surface. As shearing motion is encountered, the network of adsorbed molecules is extended and small embryonic crystallites will be formed (Fig. 2) [17]. This increases the relaxation times of the entanglement, which allows extreme extension of the chain molecules. As the chains are extended, the free energy of coiled molecules increases. It is this higher free energy that induces crystallization and at higher crystallization temperatures the chains have to be further extended before crystallization can take place, thus producing high strength & high modulus fibers.

The macroscopic structure of this fiber is shown in Fig. 3 revealing a smooth parallel structure of elementary microfibrils, which can be easily peeled off in the fiber growth direction. The grown

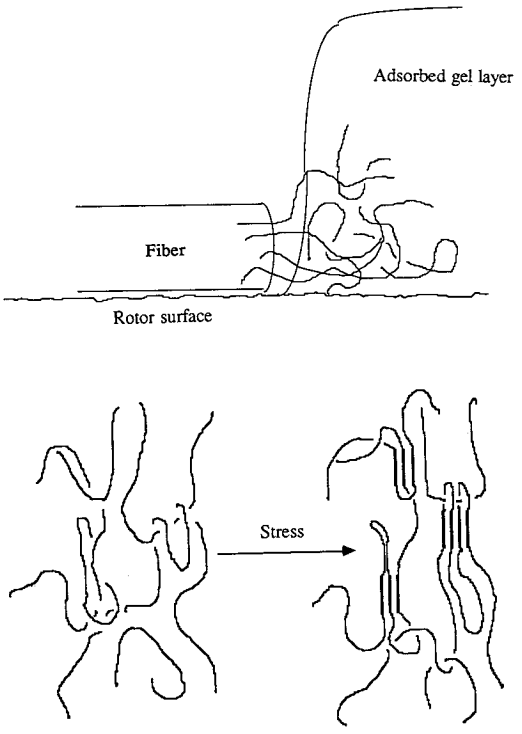

Fig. 2. (a) Schematic diagram of surface growth mechanism at rotor surface.
(b) Formation of embryonic crystallites when stess is applied.

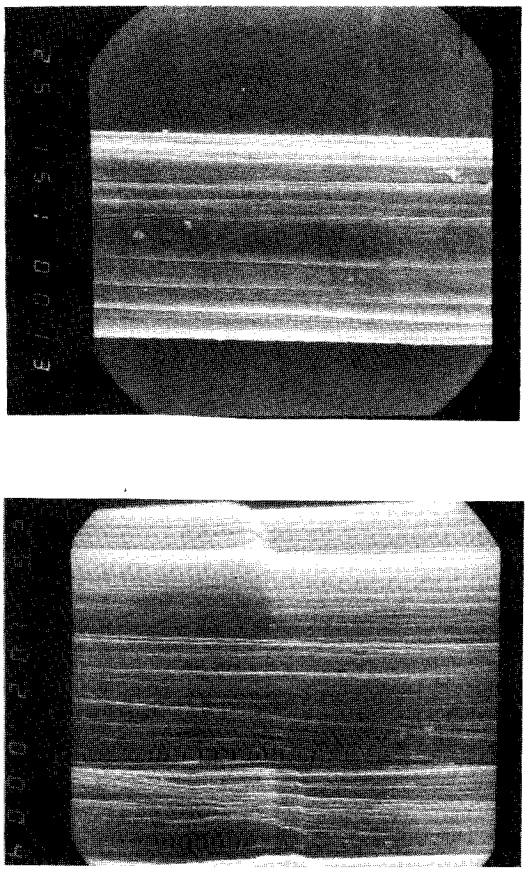

Fig. 3. (a) Typical view of surface grown fiber at optimum condition (150×).
(b) Typical view of surface grown fiber at optimum condition (1000×).

fiber show a flat ribbon like structure having a width ranging from 20 μm to 300 μm.

4. Results and Discussion

4.1. Effect of rotor speed

The birefringence measurements of surface grown fibers are shown in Fig. 4 changing the rotor speed from 20 rpm to 100 rpm which corresponds to a linear velocity of 83.7 mm/s and 418.5 mm/s, respectively. It shows a slight increase in the molecular orientation as the rotor speed is increased. This can be explained as an excess shearing motion of the gel layer and that the seed crystal can stretch the entangled molecules further, obtaining a structure with reduced trapped entanglements and amorphous regions thus leading to a more perfect structure. This is shown clearly for the tensile modulus & breaking stress results (Fig. 5 & 6) whereas both the tensile modulus & the breaking stress are linearly increasing as the rotor speed increased.

4.2. Effect of take-up speed

The heat of fusion (Fig. 7) were examined as the take-up speed was varied between 40 rpm to 120 rpm, which correspond to a linear velocity of 1.62 mm/s and 4.84 mm/s, respectively. It shows a sharp decrease at very low take-up speeds, while a slight increase at take-up speeds higher than 60 rpm. The decrease may be due to the overgrowth of the resulting fibers when the resident time of the seed is too long. It leads to a

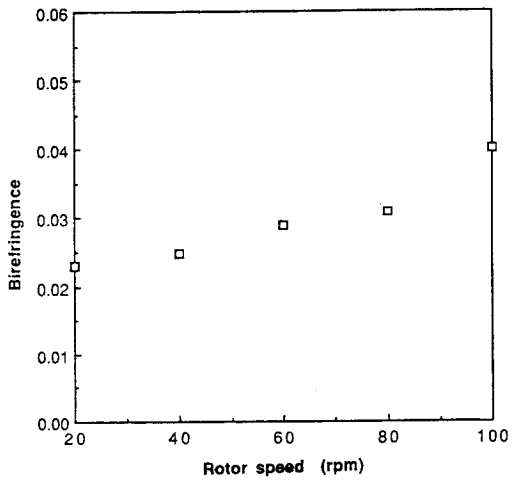

Fig. 4. Effect of rotor speed on the briefringence of surface grown fibers.

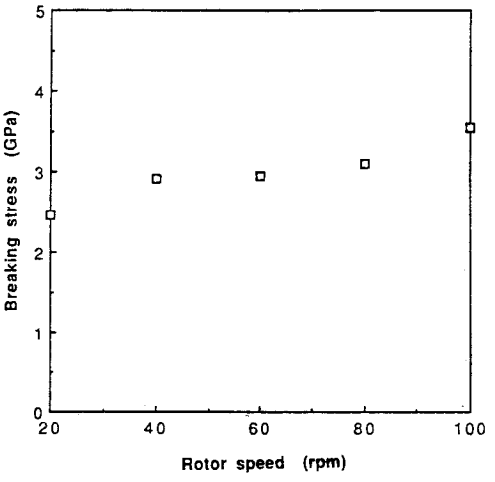

Fig. 6. Effect of rotor speed on the breaking stress of surface grown fibers.

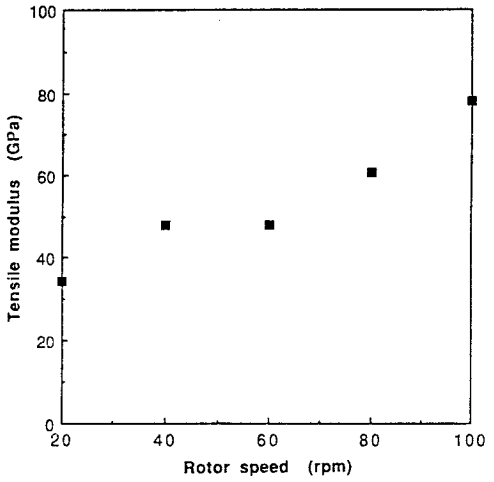

Fig. 5. Effect of rotor speed on the tensile modulus of surface grown fibers.

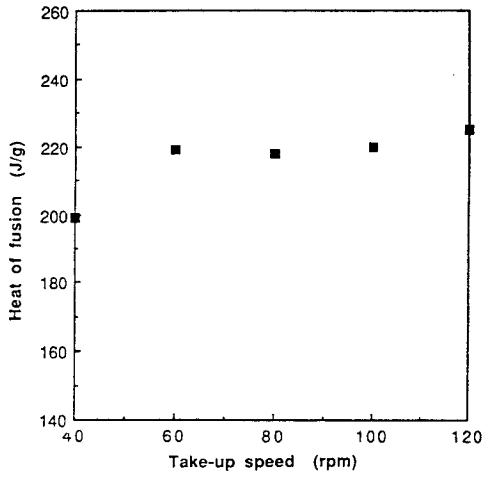

Fig. 7. Effect of take-up speed on the heat of fusion of surface grown fibers.

closed loop of grown fibers which results to a great tension & unstable conditions, thus lowering the crystallinity of the fiber. The slight increase at higher speeds are due to the slight increase of the relative linear velocity of the rotor & seed crystal, but this should not be confused with that, as the take-up speed increases the resident time of growth is shortened, thus does not give direct proportional increase to the linear velocity. During this experiment a decrease in fiber diameter as the take-up speed increased can be clearly visualized. Birefringence measurements (Fig. 8) well coincides with the above results, showing a great decrease of molecular oreintation at low take-up speeds. Tensile measurements (Fig. 9, 10) also show similar results as above.

4.3. Effects of polymer concentration

Scanning electron micrographs were taken for the fibers changing the polymer concentration

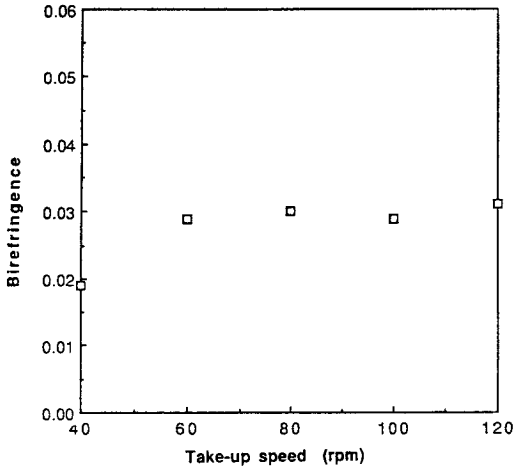

Fig. 8. Effect of take-up speed on the birefringence of surface grown fibers.

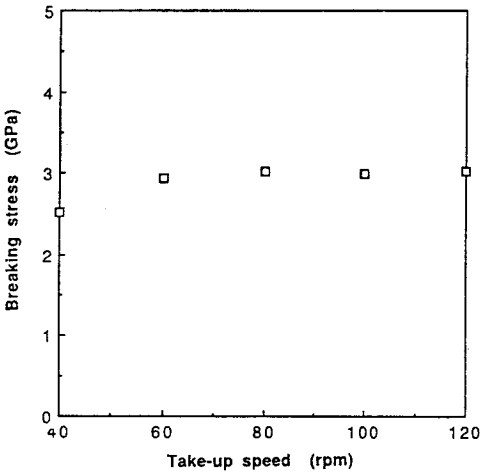

Fig. 10. Effect of take-up speed on the breaking stress of surface grown fibers.

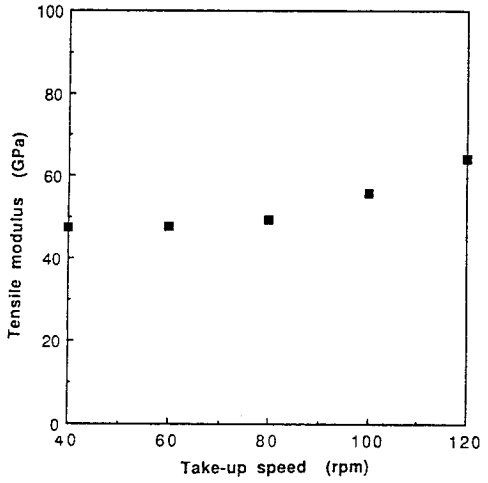

Fig. 9. Effect of take-up speed on the tensile modulus of surface grown fibers.

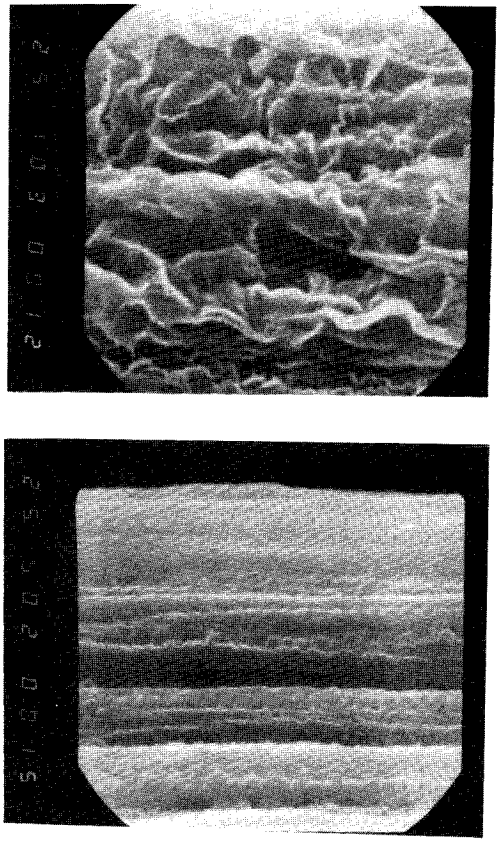

Fig. 11. (a) View of surface grown fiber at 0.4 wt.% (10000×).
(b) View of surface grown fiber at 1.0 wt.% (6000×).

(Fig. 11). It showed a somewhat porous structure at lower concentrations (0.4 wt.%). At 1.0 wt.% the surface of the fiber did not show a smoother structure compared to the fibers grown at 0.6 wt.% and 0.7 wt.% This may be due to the enormous tension between the gel layer and the seed crystals as the concentration was increased, giving an unstable growth condition resulting to frequent fracturing during the growth process.

The birefringence (Fig. 12) show similar results, giving a linear increase up to 0.7 wt.%, but a slight decrease over 0.7 wt.% revealing an increase in

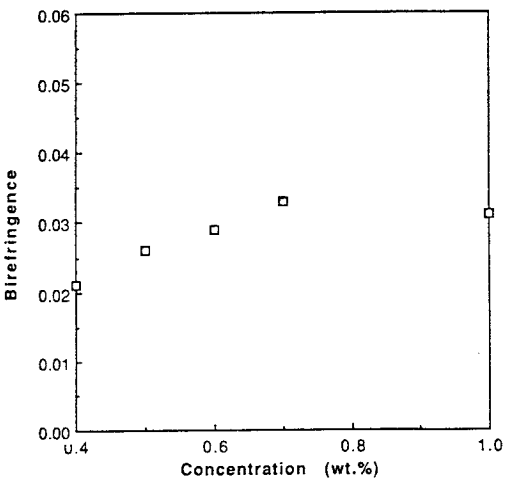

Fig. 12. Effect of concentration on the birefringence of surface grown fibers.

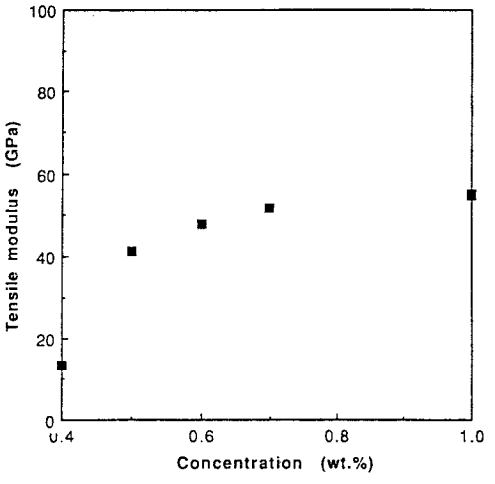

Fig. 14. Effect of concentration on the tensile modulus of surface grown fibers.

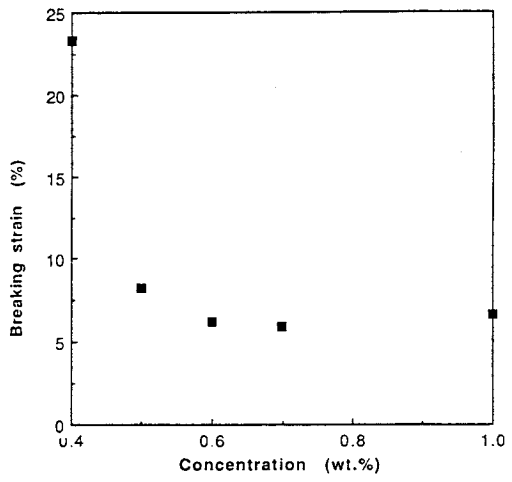

Fig. 13. Effect of concentration on the breaking strain of surface grown fibers.

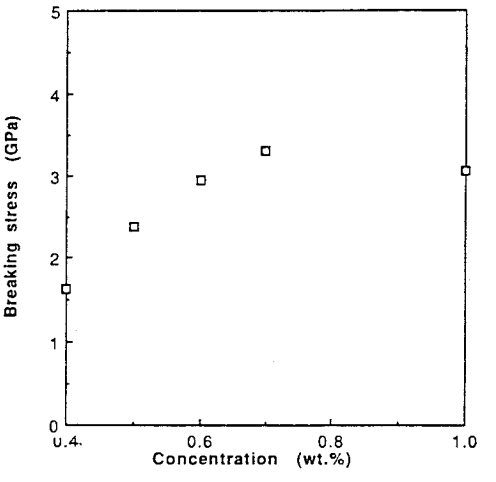

Fig. 15. Effect of concentration on the breaking stress of surface grown fibers.

the molecular orientation only up to 0.7 wt.%. The fiber grown at 0.4 wt.% showed great yielding upon deformation, giving a way high breaking strain (Fig. 13) of 23.3%, well corresponding to the porous structure of Fig. 11.

Stress-strain measurements showed similar results revealing that there is no significant modification of the mechanical properties above the concentrations of 0.7 wt.% and at concentration below 0.5 wt.%, since there is a signficant decrease of modulus & breaking stress in these concentration regions (Fig. 14 & 15). This gives a somewhat optimum condition concerning the polymer concentrations, ranging between 0.5 wt.% and 0.7 wt.%.

The data corresponding to concentrations in the range of 0.8-0.9 wt.% were not obtained due to frequent fracturing at these conditions. The effect of increasing fiber thickness followed by an increase of fiber tension cancels out each other, giving rise to this unstable condition.

4.4. Effect of crystallization temperature

Scanning electron micrographs were taken for the fibers crystallized by the suface growth technique at two different crystallization temperatures, i.e. 95℃ & 120℃. Fig. 16 shows a periodic bundle of chain-folded platelet structure crystallized at 95℃, somewhat of the shish-kebab type. As the crystallization temperature was increased the periodic platelet structure became progressively less abundant, whereas the fibrillar striations appeared perfectly smooth and parallel to the fiber growth direction at 120℃.

Birefringence measurements (Fig. 17) are plotted showing a linear increase respect to their crystallization temperature. It also shows a remarkable increase of birefringence at crystallization temperatures (120℃) above the termodynamic equilibrium temperature (118.6℃). This may be because at higher crystallization temperatures the chains have to be further extended before crystallization can take place and thus the amount of stress will be higher and smaller lamella are formed resulting in a more perfect orientation of the fiber. For reference the orientation factor f_c for the sample obtained at 120℃ was 0.975 determined by X-ray diffraction methods.

Stress-strain measurements were carried out in a temperature range of 95℃ to 120℃. At low temperatures the fiber showed quite some yielding,

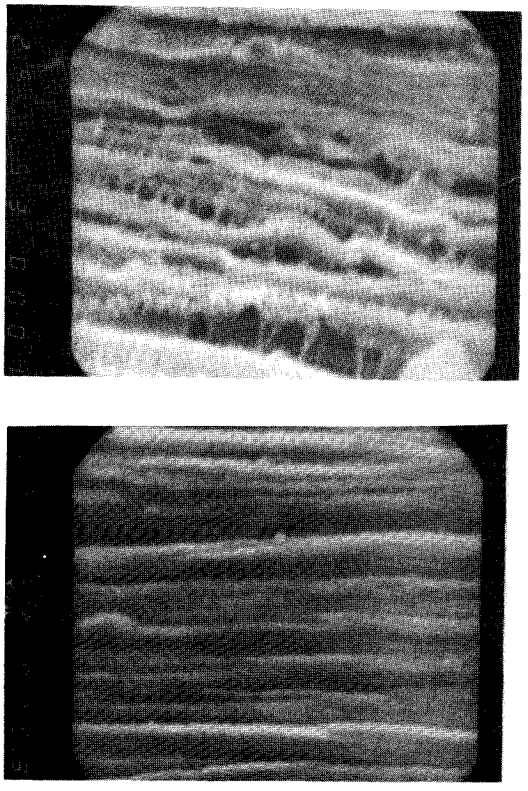

Fig. 16. (a) View of surface grown fiber at a temp. of 95℃ (15000×).
(b) View of surface grown fiber at a temp. of 120℃ (15000×).

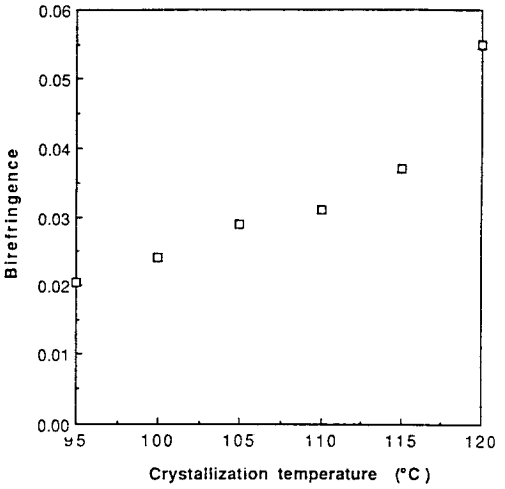

Fig. 17. Effect of crystallization temperature on the birefringence of surface grown fibers.

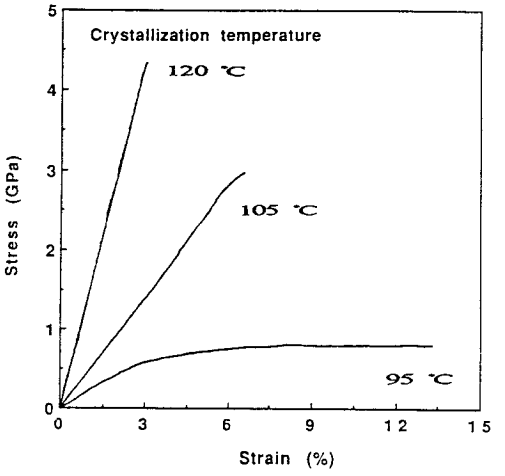

Fig. 18. Typical stress-strain curves at various crystallization temperatures.

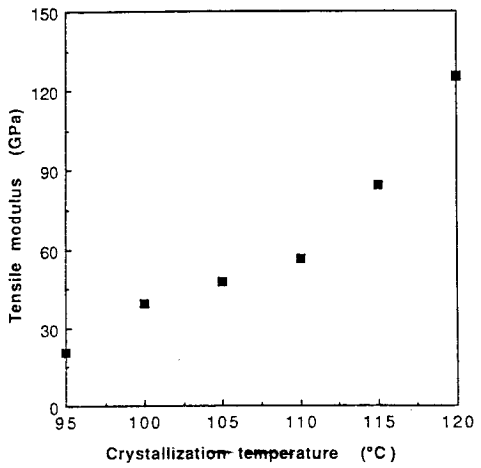

Fig. 19. Effect of crystallization temperature on the tensile modulus of surface grown fibers.

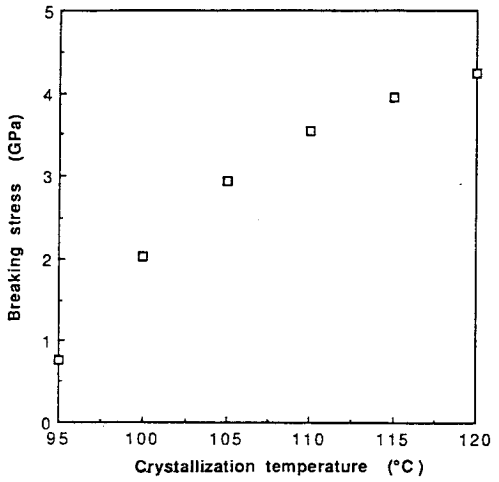

Fig. 20. Effect of crystallization temperature on the breaking stress of surface grown fibers.

probably associated with the deformation of the lamellar overgrowth. However fibers grown at higher temperatures showed a nearly Hookean behavior (Fig. 18). In Fig. 19 & 20 the tensile modulus and breaking stress are plotted against the crystallization temperature showing clearly that the crystallization temperature might be a dominant factor in determining the mechanical properties. The tensile modulus increased linearly up to 115℃, but shows a significant jump above the thermodynamic equilibrium temperature. The breaking stress showed a slight plateau above 110 ℃, probably due to defects that cannot be lessen further in the fiber. The highest tensile modulus & breaking stress achieved was 133 GPa and 5.04 GPa, respectively at a crystallization temperature of 120℃. This value is still well off range of the ideal breaking strain of 33%, tensile modulus of 340 GPa and breaking stress of 31.9 GPa calculated by quantum mechanics [22], showing the ideal arrangements of polyethylene chains in the orthorhombic lattice still have not been achieved and that stress concentrations around defects may cause some early fracturing.

5. Conclusions

UHMW PE fibers grown by the surface growth technique above the thermodynamic equilibrium temperature (118.6℃), obtained a tensile modulus of 133 GPa and a breaking stress as high as 5.04 GPa at a breaking strain of 3.1%, showing good physical properties.

The crystallization temperature was the most dominant factor affecting the physical properties of surface grown fibers and the physical properties were also well affected by changing the rotor speed, but less significant than the crystallization temperature. Changes did not encounter varying the take-up speed, but a clear decrease in physical properties in the low take-up speed regions were shown. An optimum polymer concentration range for the surface growth technique could be obtained in view of physical properties, ranging between 0.5 wt.% and 0.7 wt.%.

References

1. A.E. Zachariades, T. Kanamoto, and R.S. Porter, *J. Polym. Sci., Polym. Phys. Ed.*, **18**, 575 (1980).
2. M. Kamezawa, K. Yamada, and M. Takayanagi, *J. Appl. Polym. Sci.*, **24**, 1227 (1979).
3. T. Kunugi, A. Suzuki, and M. Hashimoto, *J. Appl. Polym. Sci.*, **26**, 213 (1981).
4. T. Kunugi, C. Ichinose, and Suzuki, *J. Apply. Polym. Sci.*, **31**, 429 (1986).

5. T. Kunugi, S. Oomori, and S. Mikami, *Polymer,* **29**, 814 (1988).
6. P. Smith, P.J. Lemstra, J.P.L. Pijpers, and A.M. Kiel, *Colloid & Polymer Sci.,* **259**, 1070 (1981).
7. P. Smith and P.J. Lemstra, *Polymer,* **21**, 1341 (1980).
8. B. Kalb and A.J. Pennings, *Polymer,* **21**, 3 (1980).
9. A.J. Pennings and K.E. Meihuizen, in "Ultra-High Modulus Polymers", I. Ward and A. Ciferri, Eds., Applied Science, Barking, Essex, England, 1979.
10. A. Keller, in "Ultra-High Modulus Polymers", I. Ward and A. Ciferri, Eds., Applied Science, Barking, Essex, England, 1979.
11. A.J. Pennings, J. Smook, J. de Boer, S. Gogolewski and van Hutten, *Pure & Appl. Chem.,* **55**, 777 (1983).
12. W. Wu and W.B. Black, *Polym. Eng. Sci.,* **19**, 1169 (1979).
13. A. Zwijnenburg and A.J. Pennings, *Colloid. Polym. Sci.,* **254**, 868 (1976).
14. P.J. Barham, A. Keller, *J. Material Sci.,* **15**, 2229 (1980).
15. P.J. Barham, A. Keller, *J. Polym. Sci., Polym. Lett. Ed.,* **17**, 591 (1979).
16. A.J. Pennings, J.M.M.A. van der Mark, and A.M. Kiel, *Kolloid, Z.Z. Polym.,* **237**, 336 (1970).
17. J.C.M. Torfs and A.J. Pennings, *J. Apply. Polym. Sci.,* **26**, 303 (1981).
18. P.J. Barham, M.J. Hill, and A. Keller, *Colloid Polym. Sci.,* **258**, 899 (1980).
19. A. Coombes and A. Keller, *J. Polym. Sci., Polym. Phys. Ed.,* **17**, 1637 (1979).
20. A.J. Pennings, J.C. Torfs, *Colloid Polym. Sci.,* **257**, 547 (1979).
21. R.S. Stein, *J. Polym. Sci.,* **31**, 327 (1958).
22. T. Shimaniuchi, M. Asahina, and S. Enomoto, *J. Polym. Sci.,* **59**, 93 (1963).